

# Micromechanics-Based Predictions on the Overall Stress-Strain Relations of Cement-Matrix Composites

Tsung-Hui Kuo<sup>1</sup>; Huang Hsing Pan<sup>2</sup>; and George J. Weng<sup>3</sup>

**Abstract:** A micromechanics-based model is proposed to determine the nonlinear stress-strain relations of cement-matrix composites at different concentrations of inclusions (aggregates). We first conducted some experiments to uncover the stress-strain behavior of the cement paste with a water-to-cement ratio of 0.45, and those of the mortar with the same cement paste but at three different volume concentrations of aggregates. The behavior of the cement paste is then simulated by Burgers' rheological model. In the development of the composite model, we extend the linear elastic response to the nonlinear one through the replacement of elastic moduli by the corresponding secant moduli. The nonlinear stress-strain curves of the cement-matrix composite are then determined from those of the cement paste and inclusions. It is shown that the predicted stress-strain curves of the mortar are in close agreement with the experimental curves up to an aggregate volume fraction of 49% or 60 wt %.

**DOI:** 10.1061/(ASCE)0733-9399(2008)134:12(1045)

**CE Database subject headings:** Mortar; Stress strain relation; Micromechanics; Predictions; Cements.

## Introduction

Although the fracture behavior of the cement-matrix composite is generally brittle, its stress-strain relation can be nonlinear, with a characteristic that is dependent on the nonlinear behavior of the cement-based binder and other factors. Several models have been proposed to describe the stress-strain behavior of the cement-matrix composite (Popovics 1973; Carreira and Chu 1985; Harsh et al. 1990; Almusallam and Alsayed 1995; Wee et al. 1996; Attard and Setung 1996). Most of these models, however, preset the influence factors, such as initial Young's modulus and peak strength, through inverse fitting of the measured composite data (Popovics 1973; Carreira and Chu 1985; Almusallam and Alsayed 1995; Attard and Setung 1996; Yi et al. 2003). As such, the composite properties were not strictly derived from the properties of the individual phases. The derived stress-strain relations of the composite, thus, cannot be used as the aggregate content changes, and for application to a new composite system, the Young's modulus and/or peak stress must be fitted again. Since concrete consists of the cement paste (or the binder) and sand stone aggregates, its properties are highly dependent upon the properties of the constituent phases, and the volume concentration and shape of the aggregates. It seems desirable that a theory that can be applied to a range of inclusion concentration and shape is developed for

the cement-matrix composite, so that the material constants involved do not have to be measured for each and every case.

This is the objective of the present study. Here, we take concrete as a composite with cement-based binder as the matrix and the aggregates as reinforcing inclusions. The nonlinear behavior of the binder and the volume concentration, shape, and elastic properties of the aggregates are the dominant factors in this process. Inclusions of the same shape but different sizes are taken to be perfectly bonded to, and homogeneously dispersed in the matrix. The matrix phase—or the binder—is to be broadly viewed as a combination of cement paste, fly ash, slag, silica fume, and other admixtures. In this way, the concrete is to be treated as a two-phase composite with an overall isotropy. The average shape of the inclusions will be grossly represented by a spheroidal shape, with an aspect ratio  $\alpha$  (the length-to-diameter ratio), so that, when  $\alpha=1$ , it is spherical, and when it approaches the limiting values of infinity and zero, it will represent very thin needles and very thin plates, respectively. In the theoretical development, the matrix will be referred to as phase 0, and the inclusions as phase 1. The volume concentration of the  $r$ th phase will be denoted by  $c_r$  ( $c_1+c_0=1$ ), and its bulk and shear moduli will be written as  $\kappa_r$  and  $\mu_r$ , respectively.

Before we proceed to develop the composite theory, we will first conduct some experiments to characterize the nonlinear behavior of the cement paste, and then use Burgers' four-parameter rheological model to model the matrix behavior. With this model, it is possible to establish the secant moduli of the matrix at a given stage of deformation. To go to the composite level, the Eshelby-Mori-Tanaka theory (Eshelby 1957; Mori and Tanaka 1973) will be invoked to determine the effective elastic moduli of the composite with randomly oriented ellipsoidal inclusions. Following a previously established procedure (Tandon and Weng 1988; Pan and Weng 1993), the linear relations will then be extended to the nonlinear regime by means of the secant-moduli approach. Unlike the elastic moduli, the secant moduli of the nonlinear binder will continue to decrease during the course of deformation, and, thus, they need to be constantly updated in order to calculate the entire stress-strain curves. Experiments will

<sup>1</sup>Teacher, Kangshan Agricultural and Industrial Vocational Senior High School, Kangshan 820, Taiwan.

<sup>2</sup>Professor, Dept. of Civil Engineering, Kaohsiung Univ. of Applied Sciences, Kaohsiung 807, Taiwan (corresponding author). E-mail: pam@cc.kuas.edu.tw

<sup>3</sup>Professor, Dept. of Mechanical and Aerospace Engineering, Rutgers Univ., New Brunswick, NJ 08903. E-mail: weng@jove.rutgers.edu

Note. Associate Editor: Dinesh R. Katti. Discussion open until May 1, 2009. Separate discussions must be submitted for individual papers. The manuscript for this paper was submitted for review and possible publication on May 5, 2006; approved on March 31, 2008. This paper is part of the *Journal of Engineering Mechanics*, Vol. 134, No. 12, December 1, 2008. ©ASCE, ISSN 0733-9399/2008/12-1045-1052/\$25.00.

**Table 1.** Measured Properties of Cement Paste and Mortar

$c_1$	$f_u$ (MPa)	$\epsilon_u$ ( $\times 10^{-3}$ )	$E$ (GPa)	$\nu$
0.0	48.23	6.22	12.47	0.173
0.29	49.80	4.22	17.80	0.165
0.38	52.25	4.15	19.48	0.163
0.49	52.90	4.09	22.03	0.161

also be conducted to test the behavior of mortar at three different aggregate concentrations, and the calculated composite results will be compared with these experiments.

### Experiments on the Behavior of Cement Paste and Mortar

First, cement paste and mortar were investigated and tested. The water-to-cement ratio ( $w/c$ ) of the cement paste was 0.45, and mortar was made from this same cement paste (matrix) but with different volume concentrations of fine aggregates (inclusions). The measured particle size of the inclusions was about 0.7–1.0 mm, a specific gravity of 2.65, and a shape similar to that of a spheroid with an aspect ratio  $\alpha = 1.13$ . The elastic bulk modulus and shear modulus of the inclusion are  $\kappa_1 = 19.46$  GPa and  $\mu_1 = 18.44$  GPa, respectively.

We have tested four kinds of mortar with the following volume fractions of aggregates:  $c_1 = 0, 0.29, 0.38,$  and  $0.49$ . The specimen size was about  $100\phi \times 200$  mm. At least six samples of each specimen were used to examine the material properties. Here, mortar at  $c_1 = 0$  also represents the cement paste. Specimens were under a uniaxial compression with a constant strain rate  $\dot{\epsilon} = 1 \times 10^{-5}/s$  when the age of the specimen reached the 28th day. The longitudinal and lateral strains were measured to plot the stress-strain curves, and to calculate the elastic moduli of the materials from ASTM C469.

The measured material properties of cement paste and mortar with different volume concentrations are recorded in Table 1. The cement paste containing  $c_1 = 0$  has the peak stress of  $f_u = 48.23$  MPa, the peak strain of  $\epsilon_u = 6.22 \times 10^{-3}$ , Poisson's ratio of  $\nu_0 = 0.173$ , and the Young's modulus of  $E_0 = 12.47$  GPa. The bulk and shear moduli of cement paste are calculated to be  $\kappa_0 = 6.37$  GPa and  $\mu_0 = 5.33$  GPa, respectively. The longitudinal stress-strain curves of the material are depicted in Fig. 1, where the solid line at each aggregate concentration is the average stress-strain curve for the samples tested for each material. From Fig. 1, mortar with increasing volume fraction of inclusions is seen to exhibit increasing Young's modulus and peak strength. For at a higher volume aggregate content such as  $c_1 = 0.6$ , there was not sufficient cement paste in the mortar to completely bind the inclusions. In this case, the theory to be developed cannot be applied.

Now we simulate the stress-strain curve at  $c_1 = 0$  in Fig. 1 to establish the constitutive equation of the cement paste with  $w/c = 0.45$ , as

$$\frac{\sigma}{f_u} = 3.71 \times [e^{-0.408\epsilon/\epsilon_u} - 1.0096e^{-0.947\epsilon/\epsilon_u}] + 0.0356 \quad (1)$$

where  $\sigma, f_u, \epsilon,$  and  $\epsilon_u$  = stress, peak stress, strain, and peak strain of the cement paste, respectively. The comparison between the experimental stress-strain curve at  $c_1 = 0$  and Eq. (1) is shown in Fig. 2. After substituting the peak strength and peak strain,

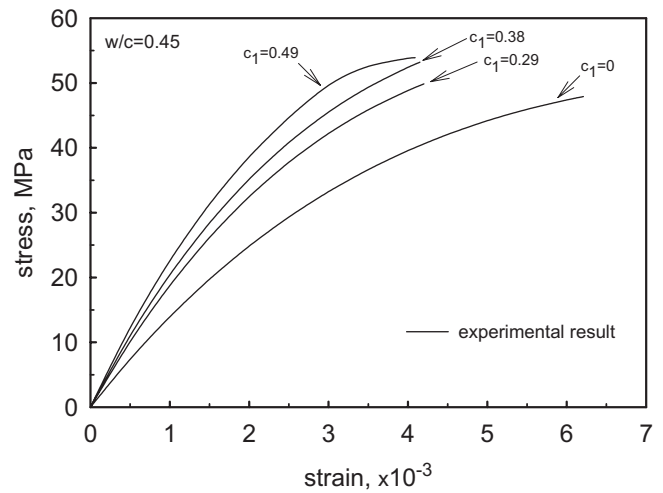


**Fig. 1.** Experimental stress-strain relations of cement-based materials with four volume concentrations of the inclusion

$f_u = 48.23$  MPa and  $\epsilon_u = 6.22 \times 10^{-3}$ , into it, one arrives at the stress-strain relation of this cement paste

$$\sigma = 178.9 \times [e^{(-0.0656)\epsilon \times 10^3} - 1.0096 e^{(-0.1523)\epsilon \times 10^3}] + 1.72 \quad (2)$$

where the unit for  $\sigma$  is MPa. For the  $100\phi \times 200$  mm specimen, the applied uniaxial compression force can be calculated by multiplying the area of the specimen into Eq. (2) to yield

$$f(\epsilon) = 1.405 \times 10^6 \times [e^{(-0.0656)\epsilon \times 10^3} - 1.0096 e^{(-0.1523)\epsilon \times 10^3}] + 1.351 \times 10^4 \quad (3)$$

where the unit of  $f(\epsilon)$  is  $N$ . One can rewrite  $f(\epsilon)$  in terms of time  $t$  by using  $\dot{\epsilon} = \epsilon/t$ , where  $\dot{\epsilon} = 10^{-5}/s$  here. It follows that

$$f(t) = 1.405 \times 10^6 \times [e^{(-0.0656)t} - 1.0096 e^{(-0.1523)t}] + 1.351 \times 10^4 \quad (4)$$

where function  $f(t)$  is the applied load as a function of time  $t$ . This form will allow us to estimate the material parameters of the binder using Burgers' four-parameter model in the next section.

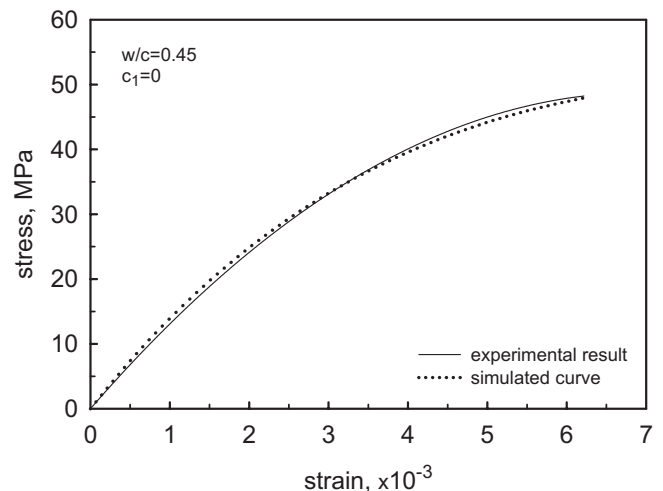


**Fig. 2.** Numerical simulation and the experimental stress-strain curve of cement paste at  $w/c = 0.45$

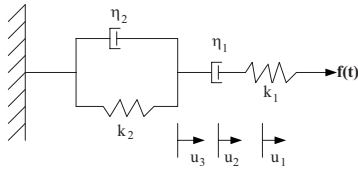


Fig. 3. Four-parameter model for cement-based binder

### Rheological Model for the Cement Paste

The stress-strain relations of cement paste or the cement-based binder are nonlinear. The nonlinearity stems from the inelastic deformation of the binder itself as well as from possible microcracking under loading (Attigbe and Darwin 1987). We tried at least 18 mechanical models, and finally found that the nonlinear behavior of the binder can be represented by Burgers' four-parameter rheological model with two springs and two dashpots, as shown in Fig. 3.

The applied load  $f(t)$  in Fig. 3 has to satisfy the constitutive relations

$$f(t) = k_1 u_1 \quad (5)$$

$$f(t) = \eta_1 \dot{u}_2 \quad (6)$$

$$f(t) = \eta_2 \dot{u}_3 + k_2 u_3 \quad (7)$$

where  $u_1$ ,  $u_2$ , and  $u_3$  = displacements at  $k_1$ ,  $\eta_1$ , and  $k_2$  and  $\eta_2$ , respectively. Noting that the velocity  $v = \dot{u} = \dot{u}_1 + \dot{u}_2 + \dot{u}_3$ , one readily arrives at the governing differential equation for this four-parameter model

$$\ddot{f}(t) + \left( \frac{k_1}{\eta_1} + \frac{k_1}{\eta_2} + \frac{k_2}{\eta_2} \right) \dot{f}(t) + \frac{k_1 k_2}{\eta_1 \eta_2} f(t) = k_1 \dot{v} + \frac{k_1 k_2}{\eta_2} v \quad (8)$$

Using a constant velocity ( $\dot{v} = 0$ ) and the initial condition  $f(0) = 0$ , the load can be expressed as

$$f(t) = b \left[ e^{m_1 t} - \left( \frac{\eta_1 v + b}{b} \right) e^{m_2 t} \right] + \eta_1 v \quad (9)$$

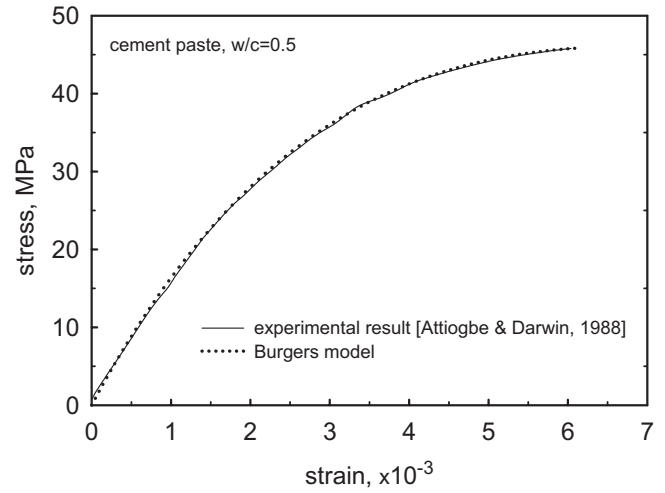
where  $b$  = constant, whereas  $m_1$  and  $m_2$  = characteristic roots satisfying the relations

$$m_1 + m_2 = - \frac{\eta_1(k_1 + k_2) + \eta_2 k_1}{\eta_1 \eta_2} \quad m_1 m_2 = \frac{k_1 k_2}{\eta_1 \eta_2} \quad (10)$$

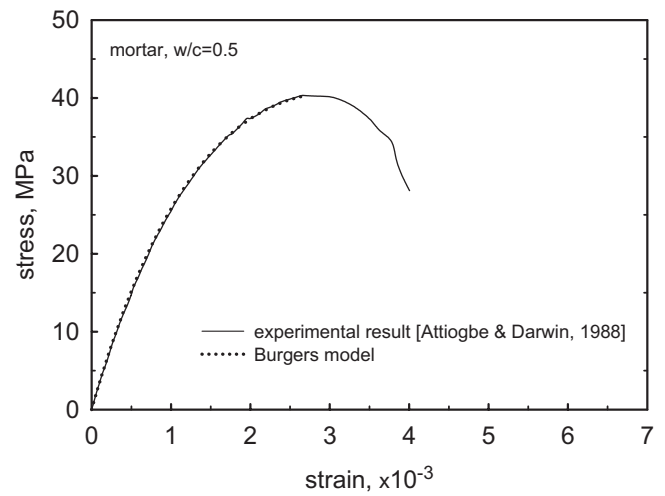
The material constants for the present cement paste are determined by comparing Eq. (9) to Eq. (4), as  $b = 1.405 \times 10^6$  N;  $m_1 = -0.0656$ ;  $m_2 = -0.1523$ ; and  $\eta_1 v = 1.351 \times 10^4$  N. The velocity applied on the specimen was  $v = \dot{u} = 2 \times 10^{-6}$  m/s, and the viscosity coefficient was found to be  $\eta_1 = 6.75 \times 10^9$  N s/m.

The initial conditions were  $u_2 = u_3 = 0$  and  $u = u_1$ . At this stage, the applied load was  $f(t) = k_1 u$ , and this led to the stress-strain relation of the cement paste satisfying Hooke's law or  $\sigma = E_i \varepsilon$  in which  $E_i$  is its initial elastic Young modulus. Thus, the spring constant has the relation  $k_1 = E_i A / L$ , where  $A$  = area of the specimen, and  $L$  = length of the extensometer. From the experimental data,  $E_i = 12.47$  GPa and  $L = 100$  mm, one has  $k_1 = 9.79 \times 10^8$  N/m.

For the other two material coefficients  $k_2$  and  $\eta_2$ , one could use the known values of  $m_1$ ,  $m_2$ ,  $k_1$ ,  $\eta_1$ , and Eq. (10). The calculated results are  $k_2 = 9.30 \times 10^9$  N/m and  $\eta_2 = 1.38 \times 10^{11}$  N s/m. By this process, the four material parameters of the cement paste with  $w/c = 0.45$  are found.



(a)



(b)

Fig. 4. Simulations of stress-strain curve of (a) cement paste; (b) mortar with  $w/c = 0.5$  by the Burger model

In light of Eq. (9), the stress-strain relation in Eq. (1) now can be recast into

$$\sigma(\varepsilon) = 3.71 f_u \times [e^{m_1 \varepsilon \times 10^3} - 1.0096 e^{m_2 \varepsilon \times 10^3}] + 0.0356 f_u \quad (11)$$

To demonstrate the wide applicability of the four-parameter model to other cement paste and even cement-based binder with different  $w/c$ , we consider the experimental data reported by Attigbe and Darwin (1988), with  $w/c = 0.5$ . This cement paste has a peak stress of 45.78 MPa; its test data are depicted by the solid line in Fig. 4(a). After determining the constants as  $k_1 = 5.8 \times 10^8$  N/m,  $k_2 = 5.8 \times 10^9$  N/m,  $\eta_1 = 3.1 \times 10^9$  N s/m,  $\eta_2 = 5.0 \times 10^{10}$  N s/m for this cement paste, the theoretical curve is also plotted alongside as a dotted line, displaying a satisfactory agreement. In fact we have found that this four-parameter model can also be used to simulate their mortar behavior whose experimental results are reproduced in Fig. 4(b). This mortar has a peak stress of 40.38 MPa. With the material constants  $k_1 = 1.9 \times 10^9$  N/m,  $k_2 = 1.6 \times 10^{10}$  N/m,  $\eta_1 = 5.0 \times 10^9$  N s/m,  $\eta_2 = 6.3 \times 10^{10}$  N s/m, the simulated curve before softening of the

mortar is also shown there (Note: Burgers model cannot be used to model the postpeak—or softening—response, and, thus, the ensuing composite model should be used to the prepeak range only). The spring and dashpot constants for the binder and the mortar are of course different. This demonstration shows that the nonlinear curves for both types of materials can be represented by the Burgers model, but for the mortar, its constants will have to be determined by simulation for each and every case as its aggregate content changes. Thus, despite its good simulation, such a curve-fitting procedure for the mortar has no predictive power. This is what prompted us to develop a micromechanics-based secant moduli method so that the nonlinear behavior of the mortar can be calculated from those of its cement paste at every volume fraction of the aggregates  $c_1$ .

### Overall Secant Moduli and the Stress-Strain Curves of Cement-Matrix Composites

The Eshelby (1957) and Mori-Tanaka (1973) theories have their established applications to the determination of effective elastic moduli of a two-phase composite containing aligned, two-dimensional (2D) or three-dimensional (3D), randomly oriented, ellipsoidal inclusions. Detailed exposition of this method can be found in Weng (1984) and Benveniste (1987), and in Tandon and Weng (1986) for both two- and three-dimensional randomly oriented spheroidal inclusions. The calculated overall elastic moduli have been shown to lie on or within the universal Hashin-Shtrikman bounds (Hashin and Shtrikman 1963; Weng 1990) for the isotropic case, and on or within the Willis anisotropic bounds (Willis 1977; Weng 1992) for the aligned configuration. The results of this method also coincide with those of the double-inclusion model when the double cells have the same shape and orientation as the enclosed inclusions (Hu and Weng 2000). With the general ellipsoidal inclusions, the explicit forms of the effective elastic moduli have also been found for monotonically aligned, 2D randomly oriented, and 3D randomly oriented arrangements (Pan and Weng 1995).

In this study, the cement-matrix composites are assumed to be isotropic containing 3D randomly oriented ellipsoidal inclusions (aggregates). In this case, the overall effective bulk and shear moduli of the two-phase composite can be respectively expressed as (Pan and Weng 1995)

$$\frac{\kappa}{\kappa_0} = \frac{1}{1 + c_1(p_2/p_1)} \quad \frac{\mu}{\mu_0} = \frac{1}{1 + c_1(q_2/q_1)} \quad (12)$$

where

$$\begin{aligned} p_1 &= 1 + c_1[b_1 + 2(b_2 + b_3 + b_4 + b_5)]/3 \\ p_2 &= (a_{11} + a_{12} + a_{13} + a_{21} + a_{22} + a_{23} + a_{31} + a_{32} + a_{33})/3 \\ q_1 &= 1 + c_1[2(b_1 - b_2 - b_3) + 7b_4 - 5b_5 + 6b_6]/15 \\ q_2 &= [3(b_{12} + b_{13} + b_{23}) + 2(a_{11} + a_{22} + a_{33}) \\ &\quad - (a_{12} + a_{13} + a_{21} + a_{23} + a_{31} + a_{32})]/15 \end{aligned} \quad (13)$$

Constants  $a_{ij}$ ,  $b_{ij}$ , and  $b_i$  are listed in the Appendix. They are functions of the volume concentration  $c_1$  of the aggregates and their shape as represented by Eshelby's  $\mathbf{S}$ -tensor, as well as the elastic bulk and shear moduli of both constituent phases.

For the calculation of nonlinear stress-strain relations of the composite, we extend the elastic moduli to the secant moduli for

the cement paste and the composite. This is the approach originally proposed by Tandon and Weng (1988). As secant moduli continue to decrease in the course of deformation, their values are smaller than their elastic counterparts, such as

$$\kappa_0^s \leq \kappa_0 \quad \mu_0^s \leq \mu_0 \quad (14)$$

where the superscript "s" stands for the secant moduli, which are the direct ratio of stress to the total strain. The secant bulk and shear moduli of the matrix are related to its secant Young's modulus  $E_0^s$  through

$$\kappa_0^s(\varepsilon) = \frac{E_0^s(\varepsilon)}{3(1 - 2\nu_0)} \quad \mu_0^s(\varepsilon) = \frac{E_0^s(\varepsilon)}{2(1 + \nu_0)} \quad (15)$$

where their dependence on the strain  $\varepsilon$  is now made explicit, and its Poisson's ratio  $\nu_0$  is assumed to remain constant [note that, even though  $\nu_0$  of the binder is taken to be constant, the secant Poisson's ratio of the concrete will change; see Eq. (21) below]. The secant Young's modulus of the cement paste at a given stage of deformation can be determined from its basic definition

$$E_0^s(\varepsilon) = \sigma(\varepsilon)/\varepsilon \quad (16)$$

In the case that aggregates take the ideal spherical shape and are purely elastic, the overall effective secant bulk and shear moduli of the composite in Eq. (12) would simplify to

$$\kappa^s = \frac{\kappa_0^s(3\kappa_1 + 4\mu_0^s) - 4c_1\mu_0^s(\kappa_0^s - \kappa_1)}{3\kappa_1 + 4\mu_0^s + 3c_1(\kappa_0^s - \kappa_1)} \quad (17)$$

$$\mu^s = \frac{\mu_0^s[5\mu_1(3\kappa_0^s + 4\mu_0^s) + c_0(\mu_0^s - \mu_1)(9\kappa_0^s + 8\mu_0^s)]}{5\mu_0^s(3\kappa_0^s + 4\mu_0^s) - 6c_0(\mu_0^s - \mu_1)(\kappa_0^s + 2\mu_0^s)} \quad (18)$$

which also give the effective elastic moduli of the composite when the superscript "s" is removed (Weng 1984). Here  $c_0 = 1 - c_1$  is the volume fraction of the binder.

When the average shape of aggregates is not spherical but rather ellipsoidal, the overall effective secant moduli can be similarly determined by replacing  $\kappa_0$  and  $\mu_0$  by  $\kappa_0^s$  and  $\mu_0^s$ , respectively, in the parameters  $a_{ij}$ ,  $b_{ij}$ , and  $b_i$ . Recasting Eq. (12) in terms of the secant moduli, we then have

$$\frac{\kappa^s}{\kappa_0^s} = \frac{1}{1 + c_1(p_2/p_1)} \quad \frac{\mu^s}{\mu_0^s} = \frac{1}{1 + c_1(q_2/q_1)} \quad (19)$$

where parameters in  $p_1$ ,  $p_2$ ,  $q_1$ , and  $q_2$  also change to their secant form.

This completes the development of the theory. To briefly recapitulate, the stress-strain curve of the cement-matrix composite at a given volume fraction of the aggregates  $c_1$  is determined as follows. First, the stress-strain curve of the cement-based binder (without the aggregates) is obtained from the experiments. The curves are then simulated by Burgers model or Eq. (11) to determine the material constants. At this stage,  $m_1$  and  $m_2$  values from the simulated curves are found, and the secant Young's modulus  $E_0^s(\varepsilon)$  can be calculated from Eq. (16), and so can the secant bulk and shear moduli of the binder from Eq. (15). The overall effective secant bulk and shear moduli of the cement-matrix composite (mortar or concrete),  $\kappa^s(\varepsilon)$  and  $\mu^s(\varepsilon)$ , follow from Eq. (19) or from Eqs. (17) and (18) if the shape of the aggregate particles is equiaxial. Finally, the overall effective secant Young's modulus of the composite is obtained from



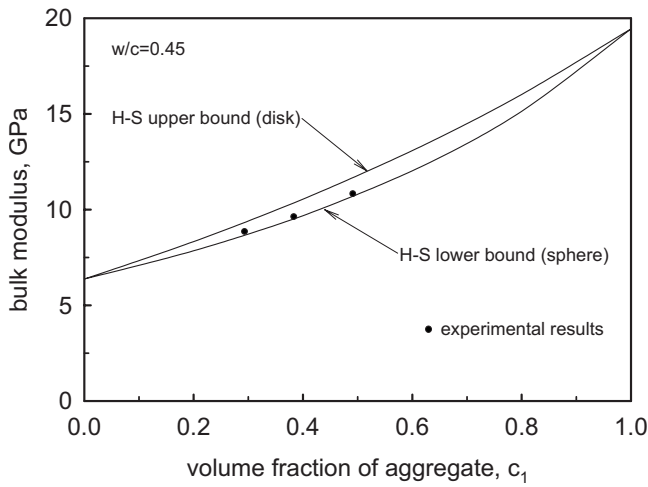


Fig. 5. Effective elastic bulk modulus of mortars

$$E^s(\varepsilon) = \frac{9\kappa^s(\varepsilon)\mu^s(\varepsilon)}{3\kappa^s(\varepsilon) + \mu^s(\varepsilon)} \quad (20)$$

Though not needed in the plot, the secant Poisson's ratio of the composite can be calculated from

$$\nu^s(\varepsilon) = \frac{3\kappa^s(\varepsilon) - 2\mu^s(\varepsilon)}{2[3\kappa^s(\varepsilon) + \mu^s(\varepsilon)]} \quad (21)$$

which increases from its initial value upon continuous deformation. Under a uniaxial compression, the stress-strain curve of the cement-matrix composite follows as

$$\bar{\sigma}(\varepsilon) = E^s(\varepsilon) \cdot \bar{\varepsilon} \quad (22)$$

which provides the desired overall stress versus strain ( $\bar{\sigma}$  versus  $\bar{\varepsilon}$ ) relations.

## Results and Discussion

### Linear Effective Elastic Moduli of the Mortar

In order to evaluate the validity of the proposed approach, we first examined the effective elastic moduli of the mortar. The elastic

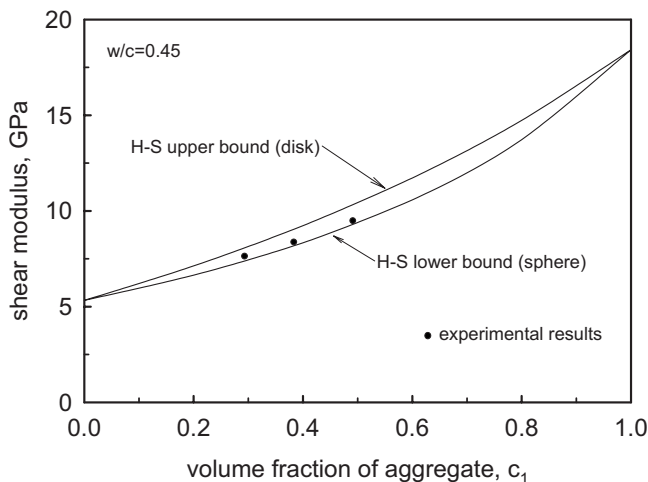


Fig. 6. Effective elastic shear modulus of mortars

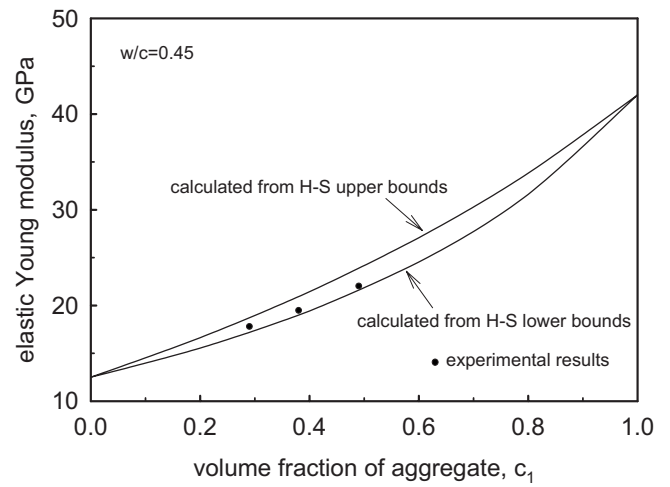


Fig. 7. Effective elastic Young's modulus of mortars

moduli of cement paste with  $w/c=0.45$  as calculated from the experiments are  $\kappa_0=6.37$  GPa and  $\mu_0=5.33$  GPa, and those of the aggregates  $\kappa_1=19.46$  GPa and  $\mu_1=18.44$  GPa. The average aspect ratio of sand was measured to be about  $\alpha=1.13$ . The measured effective bulk and shear moduli of mortar with the volume concentrations  $c_1=0.29, 0.38,$  and  $0.49$  are displayed in Figs. 5 and 6, respectively, with the circle marks. The solid lines are the Hashin-Shtrikman (H-S) upper and lower bounds, which also coincide with the extreme aspect ratios of  $\alpha \rightarrow 0$  and  $\alpha=1$ , respectively, as calculated from Eq. (12). In Figs. 5 and 6, all effective bulk and shear moduli of the mortar fall within the H-S bounds, and are also near the bound with the spherical shape ( $\alpha=1$ ). This is consistent with the well-known results that the overall effective bulk and shear moduli of the composite should fall on Hashin-Shtrikman's bounds if the inclusion shapes are of the disk and sphere shapes (Weng 1984; Tandon and Weng 1986; Benveniste 1987). We find this to be an acceptable set of data because the shape of sands  $\alpha=1.13$  is close to the sphere. Therefore, both experiment and theory for the overall elastic moduli of mortar are sufficiently accurate. To make an engineering connection, we further display the overall effective Young's modulus of mortar versus the volume concentration in Fig. 7. All experimental data are

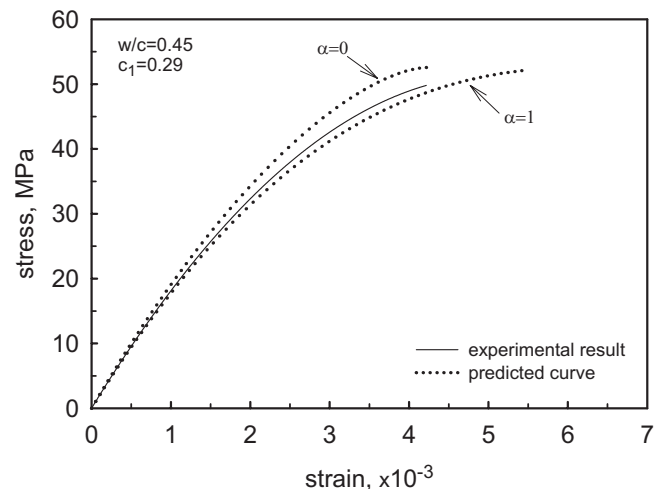
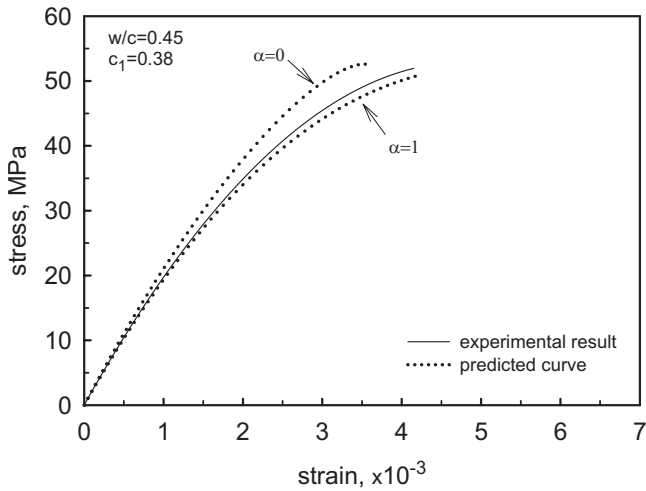


Fig. 8. Theory and experiment of the stress-strain curve of mortar at  $c_1=0.29$



**Fig. 9.** Theory and experiment of the stress-strain curve of mortar at  $c_1=0.38$

seen to lie within the curves calculated from the upper and lower bounds of the bulk and shear moduli (note that these two curves for the Young's modulus cannot be said to be bounds).

**Nonlinear Stress-Strain Curves of the Mortar at Various Concentrations of Aggregates**

From Table 1 and Fig. 1, it is evident that mortar with increasing  $c_1$  has higher elastic Young's modulus and peak stress, but has lower Poisson's ratio and peak strain. This trend persists up to  $c_1=0.49$  (or 60 wt %), beyond which the peak strength actually decreases. We have examined the samples and found that, at such a high concentration, there were insufficient binders to completely surround the aggregates. Comparison between the theory and experiment, therefore, is meaningful only up to  $c_1=0.49$  in the mortar.

The stress-strain curves of mortar with the same material properties of cement paste are calculated from the developed composite theory, and depicted in Figs. 8–10. In these figures, the solid line refers to the experimental data and the dotted lines are the predicted curves with an average inclusion aspect ratio  $\alpha \rightarrow 0$  and

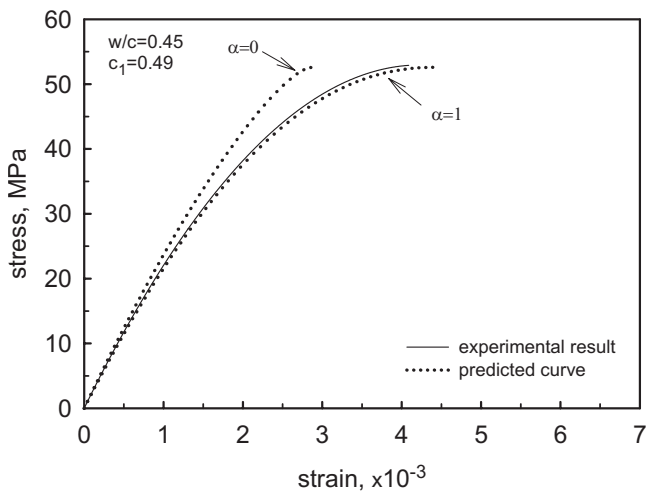


**Fig. 10.** Theory and experiment of the stress-strain curve of mortar at  $c_1=0.49$

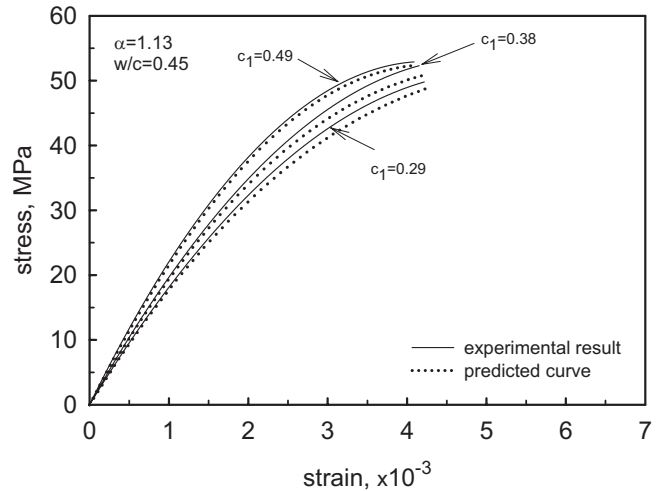


**Fig. 11.** Theory and experiment of the stress-strain curves of mortar at  $\alpha=1.13$  with the same cement paste  $w/c=0.45$

$\alpha=1$ . The results show that the experimental curves are all close to the predicted ones with the spherical shape, regardless of the volume concentration of inclusions, and are all lower than those with the disk shape ( $\alpha \rightarrow 0$ ). The theoretical predictions using the measured shape of sands at  $\alpha=1.13$  are plotted in Fig. 11, along with the three sets of experimental data. It is observed that the predicted ones are in close agreement with the test results. This agreement serves to substantiate the validity of the theory.

**Concluding Remarks**

In this paper, we have conducted some experiments to measure the nonlinear stress-strain behavior of cement-based binder and mortar at three different concentrations of aggregates, and further proposed a micromechanics-based model to predict the overall stress-strain curves of the cement-matrix composite from the properties of the cement paste and aggregate content. In the theoretical development, the nonlinear stress-strain curve of the binder was represented by the four-parameter Burgers model, from which its secant Young's modulus can be established as a function of strain. The secant moduli of the matrix are then used in the micromechanics-based composite model to find the overall secant moduli of the composite at a given concentration of inclusions. The overall nonlinear stress-strain relations of the cement-matrix composite are then determined for a given concentration of inclusions. It is found that, for the elastic behavior, the measured properties of the composite lie within the H-S bounds, and that, for the nonlinear response, the theory and experiment are in close agreement up to 49% volume concentration of inclusions or 60 wt % aggregates. The proposed theory is micromechanics based, and simple to use. It is also substantiated by experiments, and can serve as a basis for the study of other concrete properties.

**Acknowledgments**

H. H. Pan was supported by the Taiwan National Science Council under NSC 90-2211-E-151-004, and G. J. Weng was supported by the U.S. National Science Foundation, Mechanics and Structure of Materials Program, under CMS-0510409.

## Appendix

Without any summation over any repeated indices and with  $i, j, k$  always following the 1, 2, 3 even permutation, the  $a_{ij}$ ,  $b_{ij}$ , and  $b_i$  components are

$$a_{ii} = [3(\kappa_1 - \kappa_0)(\mu_1 - \mu_0)^2(S_{jjj}S_{kkkk} - S_{jjkk}S_{kkjj}) - (\mu_1 - \mu_0)(\kappa_1\mu_0 - \kappa_0\mu_1)(S_{jjjj} + S_{kkkk} - S_{jjkk} - S_{kkjj}) + 3\mu_0(\kappa_1 - \kappa_0)(\mu_1 - \mu_0)(S_{jjjj} + S_{kkkk}) + 3\kappa_0\mu_0(\mu_1 - \mu_0) + \mu_0(\kappa_1\mu_0 - \kappa_0\mu_1)]/D$$

$$a_{ij} = [3(\kappa_1 - \kappa_0)(\mu_1 - \mu_0)^2(S_{iikk}S_{kkjj} - S_{ijjj}S_{kkkk}) - (\mu_1 - \mu_0)(\kappa_1\mu_0 - \kappa_0\mu_1)(S_{iikk} + S_{kkjj} - S_{ijjj} - S_{kkkk}) - 3\mu_0(\kappa_1 - \kappa_0)(\mu_1 - \mu_0)S_{kkjj} + \mu_0(\kappa_1\mu_0 - \kappa_0\mu_1)]/D$$

$$b_{ij} = (1 - \mu_1/\mu_0)/[1 - 2S_{ijij}(1 - \mu_1/\mu_0)]$$

$$b_1 = a_{11}(S_{1111} - 1) + a_{21}S_{1122} + a_{31}S_{1133}$$

$$b_2 = [(a_{12} + a_{13})(S_{1111} - 1) + (a_{22} + a_{23})S_{1122} + (a_{32} + a_{33})S_{1133}]/2$$

$$b_3 = [a_{11}(S_{2211} + S_{3311}) + a_{21}(S_{2222} + S_{3322} - 1) + a_{31}(S_{3333} + S_{2233} - 1)]/2$$

$$b_4 = [(3a_{33} + a_{32})(S_{3333} - 1) + (3a_{23} + a_{22})S_{3322} + (3a_{13} + a_{12})S_{3311} + (3a_{32} + a_{33})S_{2233} + (3a_{22} + a_{23})(S_{2222} - 1) + (3a_{12} + a_{13})S_{2211} + 2b_{23}(2S_{2323} - 1)]/8$$

$$b_5 = [(a_{33} + 3a_{32})(S_{3333} - 1) + (a_{23} + 3a_{22})S_{3322} + (a_{13} + 3a_{12})S_{3311} + (a_{32} + 3a_{33})S_{2233} + (a_{22} + 3a_{23})(S_{2222} - 1) + (a_{12} + 3a_{13})S_{2211} - 2b_{23}(2S_{2323} - 1)]/8$$

$$b_6 = [b_{12}(2S_{1212} - 1) + b_{13}(2S_{1313} - 1)]/2$$

$$D = (\mu_1 - \mu_0)(\kappa_1\mu_0 - \kappa_0\mu_1)[S_{3333}(S_{1111} + S_{2222} - S_{1122} - S_{2211}) + S_{3322}(S_{1133} + S_{2211} - S_{1111} - S_{2233}) + S_{3311}(S_{1122} + S_{2233} - S_{1133} - S_{2222}) + S_{2211}(S_{1133} - S_{1122}) + S_{2222}(S_{1111} - S_{1133}) + S_{2233}(S_{1122} - S_{1111})] + 3(\kappa_1 - \kappa_0)(\mu_1 - \mu_0)^2[S_{3333}(S_{1122}S_{2211} - S_{1111}S_{2222}) + S_{3322}(S_{1111}S_{2233} - S_{1133}S_{2211}) + S_{3311}(S_{1133}S_{2222} - S_{1122}S_{2233})] + 3\mu_0(\kappa_1 - \kappa_0)(\mu_1 - \mu_0)(S_{1122}S_{2211} + S_{1133}S_{3311} + S_{2233}S_{3322} - S_{1111}S_{2222} - S_{2222}S_{3333} - S_{3333}S_{1111}) - \mu_0(\kappa_1\mu_0 - \kappa_0\mu_1) \times (S_{1111} + S_{1122} + S_{1133} + S_{2211} + S_{2222} + S_{2233} + S_{3311} + S_{3322} + S_{3333}) - 3\kappa_0\mu_0(\mu_1 - \mu_0)(S_{1111} + S_{2222} + S_{3333} - 1) - 3\kappa_0\mu_0\mu_1$$

## Notation

The following symbols are used in this paper:

- $A$  = area of specimen;
- $c_0$  = volume fraction of binder;
- $c_1$  = volume fraction of aggregate;
- $E$  = elastic Young's modulus of composite;

- $E_0$  = elastic Young's modulus of matrix;
- $E^s$  = effective secant Young's modulus of composite;
- $E_0^s$  = secant Young's modulus of matrix;
- $f(t)$  = applied force in terms of time  $t$ ;
- $f_u$  = peak stress;
- $L$  = gauge length;
- $\mathbf{S}$  = Eshelby's S-tensor;
- $\alpha$  = aspect ratio of aggregate;
- $\varepsilon$  = strain;
- $\bar{\varepsilon}$  = overall strain of composite;
- $\varepsilon_u$  = peak strain;
- $\kappa$  = elastic bulk modulus of composite;
- $\kappa_0$  = elastic bulk modulus of matrix;
- $\kappa_1$  = elastic bulk modulus of aggregate;
- $\kappa^s$  = effective secant bulk modulus of composite;
- $\kappa_0^s$  = secant bulk modulus of matrix;
- $\mu$  = elastic shear modulus of composite;
- $\mu_0$  = elastic shear modulus of matrix;
- $\mu_1$  = elastic shear modulus of aggregate;
- $\mu^s$  = effective secant shear modulus of composite;
- $\mu_0^s$  = secant shear modulus of matrix;
- $\nu_0$  = Poisson's ratio of matrix;
- $\sigma$  = stress; and
- $\bar{\sigma}$  = overall stress of composite.

## References

- Almusallam, T. H., and Alsayed, S. H. (1995). "Stress-strain relationship of normal, high-strength and lightweight concrete." *Mag. Concrete Res.*, 47, 39–44.
- Attard, M. M., and Setung, S. (1996). "Stress-strain relationship of confined and unconfined concrete." *ACI Mater. J.*, 93, 432–442.
- Attiogbe, E. K., and Darwin, D. (1987). "Submicrocracking in cement paste and mortar." *ACI Mater. J.*, 84, 491–500.
- Attiogbe, E. K., and Darwin, D. (1988). "Strain due to submicrocracking in cement paste and mortar." *ACI Mater. J.*, 85, 3–11.
- Benveniste, Y. (1987). "A new approach to the application of Mori-Tanaka theory in composite materials." *Mech. Mater.*, 6, 147–157.
- Carreira, D. J., and Chu, K. H. (1985). "Stress-strain relationship for plain concrete in compression." *ACI J.*, 82, 797–804.
- Eshelby, J. D. (1957). "The determination of the elastic field of an ellipsoidal inclusion, and related problems." *Proc. R. Soc. London, Ser. A*, 241, 376–396.
- Harsh, S., Shen, Z., and Darwin, D. (1990). "Stress-rate sensitive behavior of cement paste and mortar in compression." *ACI Mater. J.*, 87, 508–515.
- Hashin, Z., and Shtrikman, S. (1963). "A variational approach to the theory of the elastic behaviour of multiphase materials." *J. Mech. Phys. Solids*, 11, 127–140.
- Hu, G. K., and Weng, G. J. (2000). "The connections between the double-inclusion model and the Ponte Castaneda-Wills, Mori-Tanaka, and Kuster-Toksoz models." *Mech. Mater.*, 32, 495–503.
- Mori, T., and Tanaka, K. (1973). "Average stress in matrix and average elastic energy of materials with misfitting inclusions." *Acta Metall.*, 21, 571–574.
- Pan, H. H., and Weng, G. J. (1993). "Determination of transient and steady-state creep of metal-matrix composites by a secant moduli method." *Composites Eng.*, 3, 661–674.
- Pan, H. H., and Weng, G. J. (1995). "Elastic moduli of heterogeneous solids with ellipsoidal inclusions and elliptic cracks." *Acta Mech.*, 110, 73–94.
- Popovics, S. (1973). "A numerical approach to the complete stress-strain curve of concrete." *Cem. Concr. Res.*, 3, 583–599.
- Tandon, G. P., and Weng, G. J. (1986). "Average stress in the matrix and

- effective moduli of randomly oriented composites." *Compos. Sci. Technol.*, 27, 111–132.
- Tandon, G. P., and Weng, G. J. (1988). "A theory of particle-reinforced plasticity." *J. Appl. Mech.*, 110, 126–135.
- Wee, T. H., Chin, M. S., and Mansur, M. A. (1996). "Stress-stress relationship of high-strength concrete in compression." *J. Mater. Civ. Eng.*, 8(2), 70–76.
- Weng, G. J. (1984). "Some elastic properties of reinforced solids, with special reference to isotropic ones containing spherical inclusion." *Int. J. Eng. Sci.*, 22, 845–856.
- Weng, G. J. (1990). "The theoretical connections between Mori-Tanaka's theory and the Hashin-Shtriman bounds." *Int. J. Eng. Sci.*, 28, 1111–1120.
- Weng, G. J. (1992). "Explicit evaluation of Willis' bounds with ellipsoidal inclusions." *Int. J. Eng. Sci.*, 30, 83–92.
- Willis, J. R. (1977). "Bounds and self-consistent estimates for the overall properties of anisotropic composites." *J. Mech. Phys. Solids*, 25, 185–202.
- Yi, S. T., Kim, J. K., and Oh, T. K. (2003). "Effect of strength and age on the stress-strain curves of concrete specimens." *Cem. Concr. Res.*, 33, 1235–1244.